Photocatalytic Oxidation of Phenolic Compounds by Using a Carbon Nanotube–Titanium Dioxide Composite Catalyst

ARTICLE *in* CHEMSUSCHEM · MAY 2010

Impact Factor: 7.66 · DOI: 10.1002/cssc.200900262 · Source: PubMed

2 AUTHORS:

Cláudia Gomes Silva
University of Porto
44 PUBLICATIONS **1,606** CITATIONS
SEE PROFILE

Joaquim Luís Faria
University of Porto
170 PUBLICATIONS **3,558** CITATIONS
SEE PROFILE

DOI: 10.1002/cssc.200900262

Photocatalytic Oxidation of Phenolic Compounds by Using a Carbon Nanotube-Titanium Dioxide Composite Catalyst

Cláudia Gomes Silva and Joaquim Luís Faria*[a]

A nanostructured multiwalled carbon nanotube (CNT) and titanium dioxide composite catalyst is prepared by a modified acid-catalyzed sol–gel method. Pure anatase TiO_2 and the CNT-TiO_2 composite are tested in the photocatalytic degradation of four *para*-substituted phenols: 4-chlorophenol, 4-aminophenol, 4-hydroxybenzoic acid and 4-nitrophenol. The effect of several operational parameters on the photoefficiency of the composite catalyst is studied by using 4-chlorophenol as model compound, namely catalyst loading, pH of the medium, hydrogen peroxide concentration, substrate concentration. A relationship between the Hammett constant of each *para*-substituted phenolic compound and its degradability by the photocatalysts is found. The effect of the carbon phase in the catalyst is ascribed to its photosensitizer action. A clear beneficial effect is observed for the degradation of 4-aminophenol and 4-chlorophenol. For the molecules with stronger electron-withdrawing (deactivating) groups, such as 4-hydroxybenzoic acid and 4-nitrophenol, no synergy effect is observed.

Introduction

The exponential growth of the human population and the intensification of agricultural and industrial activities have resulted in a continuous increase in the demand for Earth's limited supply of fresh water. The protection of natural water resources and the development of new technologies for (waste)water treatment are key environmental issues for the 21st century.

Advanced oxidation processes (AOPs), including the Fenton and photo-Fenton processes, ozone and/or peroxide photolysis, and semiconductor photocatalysis,[1–4] are considered promising and competitive solutions for the abatement of numerous hazardous compounds in wastewater streams. AOPs are based on nonselective, highly reactive hydroxyl radicals, able to drive oxidation processes that lead to the complete elimination and full mineralization of a wide range of organic and inorganic pollutants. The importance of photocatalytic processes that use semiconductor catalysts for wastewater treatment has increased, because they are among the most effective breakdown technologies.[5,6] What contributes to this status is that these processes require only mild operating conditions and in many cases result in total mineralization of the pollutants, without any additional waste disposal problems.

TiO_2 has been extensively employed as photocatalyst in wastewater treatment by oxidative degradation.[5,7] The photocatalytic activity of TiO_2 largely depends on its microstructure and physical properties[8–10] as well as on the incorporation of some other metal ions, adsorbents, or supports.[11–13] It has been reported that carbon materials have some beneficial effects on the photocatalytic activity of TiO_2 by inducing synergies or cooperative effects between the metal oxide and carbon phases.[14–17] Since they were discovered,[18] carbon nanotubes (CNTs) have been the focus of various studies owing to their unique structural, electronic, and mechanical properties. In the field of catalysis carbon nanotubes constitute a promising alternative catalyst support, competing with activated carbon.[19] Some recent works have emphasized the preparation of CNT/TiO_2 nanocomposite catalysts, aiming at a synergetic combination of their intrinsic properties and thereby enhancing performance to meet new requirements imposed by advanced applications in distinct fields, such as optoelectronics, solar energy utilization, and heterogeneous photocatalysis.[16,20–26]

In the present work, TiO_2 and a multiwalled CNT/TiO_2 composite catalyst (CNT-TiO_2) are produced by an acid-catalyzed sol–gel technique starting from an alkoxide precursor. The catalysts are used for the photocatalytic degradation of four *para*-substituted phenols (4-chlorophenol, 4-aminophenol, 4-hydroxybenzoic acid, and 4-nitrophenol) under near-UV to visible irradiation. Phenol and phenolic derivatives are common compounds in industrial wastewaters,[27–29] being refractory and recalcitrant species in conventional biological treatment processes. The heterogeneous photocatalytic process using the hybrid CNT-TiO_2 catalyst is characterized by studying the effect of several operational parameters, such as catalyst loading, pH of the reaction medium, addition of hydrogen peroxide, and substrate concentration, in the photoefficiency of degradation of 4-chlorophenol as model compound. The effect of the electronic nature of the substituent group on the photoreactivity of the *para*-substituted phenols using both TiO_2 and CNT-TiO_2 catalysts is also reported.

[a] *Dr. C. G. Silva, Prof. J. L. Faria*
Laboratório de Catálise e Materiais
Laboratório Associado LSRE/LCM
Departamento de Engenharia Química—Faculdade de Engenharia
Universidade do Porto (Portugal)
Fax: (+351) 225 081 449
E-mail: jlfaria@fe.up.pt

Results and Discussion

Catalyst characterization

X-ray diffraction (XRD) patterns of neat CNTs, TiO_2, the CNT-TiO_2 composite, and a mixture of CNT and TiO_2 powders (CNT+TiO_2) are shown in Figure 1. The CNT+TiO_2 sample was

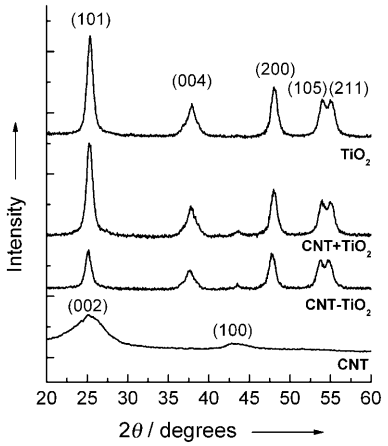

Figure 1. XRD patterns of CNTs, TiO_2, the CNT-TiO_2 composite, and the CNT+TiO_2 mixture.

prepared by mechanically mixing CNT and TiO_2 powders, maintaining the same mass ratio as for the CNT-TiO_2 preparation. With the pure CNTs, characteristic peaks corresponding to (002) and (100) reflection planes can be identified. In the neat TiO_2 and composite catalyst samples, only the anatase phase can be identified. A remarkable concurrence between the XRD patterns of TiO_2 and the CNT+TiO_2 mixture was observed. However, in the case of the CNT-TiO_2 composite catalyst, a decrease in the intensity of the peak corresponding to the (101) reflection plane could be observed, which may indicate a less-extensive crystallization of the TiO_2 crystallites through this growing face. The dimensions of the anatase crystallites ($d_{anatase}$), listed in Table 1, were determined by the diffraction broadening of the (200) reflection plane from anatase ($2\theta = 48.1^\circ$), where there is no interference from CNT, by using Scherrer's equation.[30] The anatase crystallite sizes of composite catalysts slightly decreased from 8.5 to 8.3 nm for the TiO_2 and CNT-TiO_2 catalysts, respectively. The introduction of CNTs seemed to avoid particle agglomeration, and therefore the crystallites tended to get smaller. Some studies using similar materials have shown that increasing amounts of CNTs result in a progressive decrease of the dimensions of TiO_2 crystallites.[16,24,25]

Table 1. Surface area (S), carbon load [determined by TG analysis (C_{TG})], and anatase crystallite dimension ($d_{anatase}$) of the catalyst materials.

Catalyst	S [$m^2 g^{-1}$]	C_{TG} [%]	$d_{anatase}$ [nm]
CNT	185	n.a.[a]	n.a.[a]
TiO_2	107	n.a.[a]	8.5
CNT-TiO_2	131	14.4	8.3

[a] Not applicable.

The N_2 adsorption–desorption isotherms of the CNT and CNT-TiO_2 composite catalysts can be classified as Type IV (data not shown),[31,32] indicating a mesoporous pore structure. The Brunauer–Emmett–Teller (BET) surface areas (S) of the prepared catalysts are listed in Table 1. The surface area of the composite catalyst appears to be higher than the one estimated based on the TiO_2 and CNT contents (120 $m^2 g^{-1}$). For the CNT-TiO_2 composite material, the presence of CNTs seems to prevent the TiO_2 particles from agglomerating, thus increasing the surface area.

A scanning electron microscopy (SEM) image of the CNT-TiO_2 composite material (Figure 2a) shows CNTs embedded in the TiO_2 matrix, with relatively homogeneous TiO_2 supported

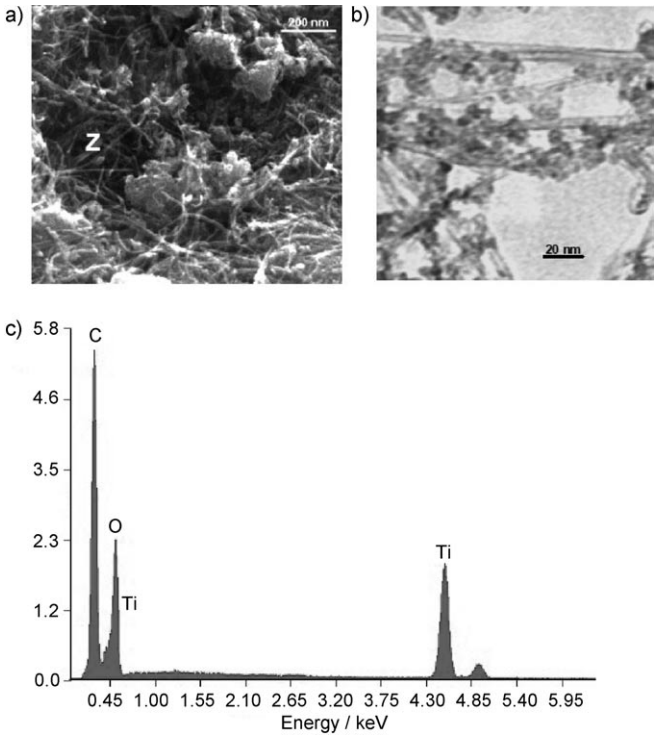

Figure 2. a) SEM and b) TEM images of the CNT-TiO_2 composite catalyst. c) EDX spectrum obtained from analysis of the CNT-TiO_2 composite catalyst in the zone labeled "Z" in the SEM image (a).

on the CNTs without apparent agglomeration of the TiO_2 particles. A transmission electron microscopy (TEM) image at a higher magnification reveals the presence of TiO_2 nanoparticles at the CNT surfaces (Figure 2b). Additionally, energy-dispersive X-ray (EDX) spectroscopy of the CNT-TiO_2 composite catalyst confirms the presence of C, O, and Ti (Figure 2c).

Based on the characterization mentioned above, the fact that the surface area of the CNT-TiO_2 composite is higher than the calculated value suggests that there may be a strong interphase structural effect between the carbon and metal oxide phases. The disappearance of the characteristic CNT peak in the XRD patterns of the composite material is in line with a homogeneous coverage of the CNT surface by TiO_2, which is also

supported by the SEM and TEM analysis. On the other hand, the introduction of CNTs seems to favor less-extensive crystallized TiO_2 domains on the CNT surface, avoiding agglomeration of TiO_2 particles.[24]

Photocatalytic degradation of 4-chlorophenol

Heterogeneous photocatalytic reactions are influenced by several parameters, such as catalyst loading, the nature and concentration of the substrate, pH of the medium, and the presence of oxidant species.[33] 4-Chlorophenol (CP) was chosen as model compound to study the effect of key operational parameters on photodegradation with the CNT-TiO_2 composite catalyst. Preliminary experiments revealed that the photocatalytic oxidation of 4-chlorophenol follows a pseudo-first-order kinetic rate model, as described by the following equation:

$$C_{CP} = C_{0,CP}e^{-k_{app}t} \quad (1)$$

where C_{CP} is the CP concentration, k_{app} is the apparent first-order kinetic constant, t is the reaction time, and $C_{0,CP}$ is the phenol concentration at $t=0$ (i.e., when the illumination is switched on). Operational parameters were therefore evaluated by comparing the values of k_{app}, obtained by nonlinear regression of the experimental data, conversion of substrate, and total organic carbon (TOC) removal measurements.

Effect of catalyst loading

The rate of photocatalytic reaction is strongly influenced by the concentration of the catalyst in the reaction medium. In heterogeneous photocatalysis, the reaction rate is known to increase proportionally to the concentration of the catalyst. The optimal loading is generally determined in order to avoid the use of excess catalyst and to ensure the efficient, total absorption of photons. A catalyst overload can cause unfavorable light scattering and reduction of light penetration into the solution.

In the present study the concentration of the CNT-TiO_2 catalyst was varied from 250 mg L^{-1} to 1.5 g L^{-1} (Table 2). Increasing the loading from 250 mg L^{-1} to 1.2 g L^{-1} led to a 20% increase in k_{app}, which supports the heterogeneous photocatalytic nature of the process. Further increasing the loading did not increase k_{app}, which can be directly related to a decrease of the number of illuminated active sites in these particular conditions. The results obtained in terms of conversion of CP ($X_{CP,2h}$) and total organic carbon removal ($X_{TOC,2h}$) at the end of the photocatalytic reactions are consistent with evaluations based on the kinetic parameter (Table 2). A maximum conversion of 72.3% after 2 h of irradiation was obtained when a 1.2 g L^{-1} catalyst loading was used, resulting in the mineralization of 47.5% of the organic matter present in the solution at the beginning of the reaction.

Table 2. First-order apparent rate constant (k_{app}), conversion ($X_{CP,2h}$), and TOC removal ($X_{TOC,2h}$) after 2 h of irradiation for the photocatalytic degradation of 4-chlorophenol ($pH_{initial}=5.60$).

$C_{CNT\text{-}TiO2}$ [g L^{-1}]	k_{app} [$\times 10^{-2}$ min^{-1}]	$X_{CP,2h}$ [%]	$X_{TOC,2h}$ [%]
0	0.607	53.7	2.18
0.25	0.864	63.7	14.0
0.50	0.930	68.7	35.4
0.80	1.003	71.4	45.7
1.2	1.039	72.3	47.5
1.5	0.990	70.2	45.9

Even without catalyst (i.e., a pure photochemical reaction), considerable degradation of CP occurred. However under these conditions TOC removal was very low, with only 2% of the organic content being removed. Although CP can be oxidized by near-UV to visible light, at the end of the reaction most of the reaction intermediates were still present in the solution. Based on these observations the amount of CNT-TiO_2 in subsequent photocatalytic degradation experiments was kept at the optimum value of 1.2 g L^{-1}.

Effect of the pH of the medium

The effect of pH on the efficiency of a photocatalytic reaction is normally a result of a combination of three main factors: (1) the surface charge of the catalyst, which is related to the acid/base properties of chemical groups at the surface of the solid material; (2) the electronic nature of the substrate (redox potential, pK_a); and (3) the abundance of H^+ or HO^- in solution, which is related to the extent of formation of hydroxyl radicals. When using TiO_2-based materials, the first aspect is related to the amphoteric behavior of TiO_2 in aqueous media. The point of zero charge (pzc) of TiO_2, that is, the point at which the surface charge density is zero, is known to be approximately 6.0.[34] At pH values higher than pH_{pzc}, the TiO_2 surface is negatively charged and TiO^- appears to be the predominant form. For lower pH values, the TiO_2 surface is in the protonated form ($TiOH_2^+$). During the sol–gel production of the CNT-TiO_2 composite, the linkage between the carbon nanotubes and titania is believed to occur between hydroxyl groups in the titania polymeric chain and carboxylic acid groups present at the surface of the CNTs.[35] The removal of some of the hydroxyl groups from titania and the presence of a carbon phase with acidic groups at its surface are expected to produce some decrease in the pH_{pzc} of the resulting composite material. The electric charge properties of both catalyst and substrate have been found to play an important role in the adsorption process. In aqueous media, 4-chlorophenol shows a pK_a of 9.41 (at 25 °C). This means that it is in the molecular form for $pH < pK_a$ while at $pH > pK_a$ the molecule undergoes deprotonation and becomes negatively charged.

The effect of pH on the photocatalytic degradation of CP was investigated for three pH values: 3.0, 5.6 (natural pH), and 11.0. The pH of the solution was adjusted before irradiation and was not controlled during the course of the reaction. As can be seen in Figure 3, an increase in pH resulted in an enhancement in the photocatalytic degradation of CP.

At pH 11.0, CP was almost totally converted after two hours of irradiation. However, under these conditions only very low mineralization of the organic compounds in solution was ach-

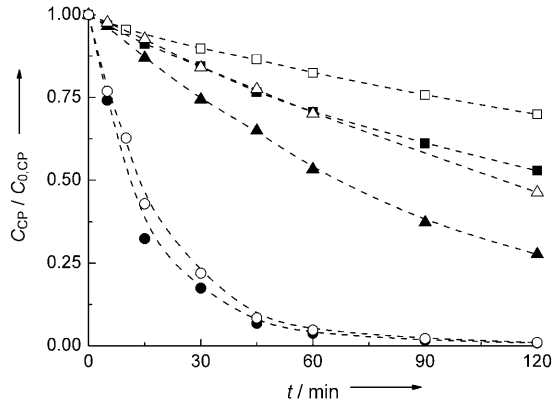

Figure 3. Evolution of the dimensionless concentration of CP during the photodegradation under different initial pH values. Filled symbols correspond to photocatalytic reactions and empty symbols to photolytic reactions; squares: pH 3.0; triangles: pH 5.6; circles: pH 11.0.

ieved (Table 3). At pH 11.0 ($pH > pK_a$), the anionic form of CP is predominant and a bathochromic shift of 18 nm was observed in the UV/Vis spectra. Therefore, a more important contribution of the photolytic process was expected to occur. In addition, at this pH auto-oxidation of CP can occur, with the formation of more-stable polymeric compounds (brownish particles were visible in solution), which accounts for the very low TOC removal. Moreover, at pH 11.0 the catalyst surface is negatively charged and the CP molecule is in its anionic form. Therefore, repulsive forces exist between the catalyst surface and the substrate, which was proved by the small amount of CP adsorbed during the dark adsorption period (see C_0 in Table 3). In this case, the fast removal of CP is attributed to a high amount of OH^- ions in the reaction medium favoring the formation of $HO^\bullet$ radicals which attack CP molecule. As can be observed in Figure 3, for initial pH of 11.0, photochemical and photocatalytic removal of CP are almost coincident. However, in the absence of catalyst no TOC removal was observed, meaning that CP was converted into organic intermediates that were not degraded.

Table 3. Effect of initial pH on the apparent rate constant (k_{app}), CP conversion ($X_{CP,2h}$) and TOC removal ($X_{TOC,2h}$) after 2 h of irradiation for the photocatalytic degradation of CP.

$pH_{initial}$	C_0 [mg L^{-1}]	k_{app} [$\times 10^{-2}$ min^{-1}]	$X_{CP,2h}$ [%]	$X_{TOC,2h}$ [%]
3.0	39.1	0.553	47.1	26.1
5.6	44.0	1.039	72.3	47.5
11.0	46.7	5.510	99.1	8.85

On the other hand, at pH 3.0 there was a significant amount of CP that was adsorbed by the catalyst during the dark adsorption period, producing a nearly 20% decrease in the concentration of the organic molecule. Under these conditions CP is present in its molecular form and the catalyst is positively charged. Simultaneously, as there is a predominance of H^+ species in solution rather than hydroxide anions, low amounts of hydroxyl radicals are generated, decreasing the rate of degradation of CP. Also, CP can be photochemically degraded under these pH conditions. Only a 4.37% TOC removal was obtained, contrasting with the 26.1% achieved in the photocatalytic reaction.

At an initial pH of 5.6, although k_{app} and CP conversion were not as favorable as under basic conditions, a higher TOC removal was achieved. In this case, CP was moderately adsorbed by the CNT-TiO_2 catalyst. To establish a compromise between kinetic and mineralization photo-efficiency it was decided to proceed with further CP degradation studies at natural pH conditions.

Addition of hydrogen peroxide

The effect of the addition of hydrogen peroxide on the efficiency of the photocatalytic degradation of CP was studied by varying the concentration of H_2O_2 in the suspensions. Pioneering works on the use of H_2O_2 in photocatalytic oxidation reactions using TiO_2 as catalyst have reported a beneficial effect caused by the introduction of the peroxide, which was attributed to its action as electron acceptor, preventing electron–hole recombination and thereby increasing the efficiency of the photocatalytic process.[36,37] However, some studies have reported that the presence of H_2O_2 at certain concentrations negatively affects the efficiency of the photocatalytic reactions, by inhibiting the formation of hydroxyl radicals.[38,39]

In this work, we varied the concentration of H_2O_2 from 0 to 30 mM. It was observed that the addition of a small amount of H_2O_2 into the reaction system produced a decrease in the apparent rate constant (Table 4).

The observed decrease in k_{app} may indicate the existence of competing mechanisms,[38,39] with hydrogen peroxide acting as: (1) electron acceptor [Equation (2)], (2) hydroxyl radical producer [Equations (3) and (4)], (3) positive hole scavenger [Equations (5) and (6)], or (4) hydroxyl radical scavenger [Equation (7)].

Table 4. Effect of H_2O_2 concentration (C_{H2O2}) on the photocatalytic degradation of CP.

C_{H2O2} [mM]	$pH_{initial}$	k_{app} [$\times 10^{-2}$ min^{-1}]	$X_{CP,2h}$ [%]	$X_{TOC,2h}$ [%]
0	5.60	1.039	72.3	47.5
3	5.50	0.580	49.7	20.0
10	5.10	0.960	68.2	26.0
30	4.90	1.080	72.8	30.2

$$H_2O_2 + e^- \rightarrow OH^- + HO^\bullet \quad (2)$$

$$H_2O_2 + O_2^{\bullet-} \rightarrow HO^\bullet + OH^- + O_2 \quad (3)$$

$$H_2O_2 \xrightarrow{h\nu} 2HO^\bullet \quad (4)$$

$$H_2O_2 + 2h^+ \rightarrow 2H^+ + O_2 \quad (5)$$

$$H_2O_2 + h^+ \rightarrow HO_2^\bullet + H^+ \quad (6)$$

$$H_2O_2 + HO^\bullet \rightarrow H_2O + HO_2^\bullet \quad (7)$$

In the presence of low amounts of hydrogen peroxide, the reaction described in Equation (4) is not expected to be the most important, because H_2O_2 shows a fair absorption of light within the working wavelength range. At low concentrations, hydrogen peroxide may adsorb on the catalyst surface and react with positive holes [Equations (5) and (6)], inhibiting the formation of hydroxyl radicals. Moreover, H_2O_2 can react with hydroxyl radicals in both adsorbed and bulk phases [Equation (7)]. These two processes may negatively affect the concentration of hydroxyl radicals and the rate of CP degradation. As the H_2O_2 concentration increases mechanisms (1) and (2) progressively start to increase in importance, and hydroxyl radical formation by the processes described by Equations (2) and (3) can in part compensate for the reduction in hydroxyl radical concentration. Therefore, the kinetic rate constant tends to increase with further addition of hydrogen peroxide to the CNT-TiO_2 slurry.

Effect of CP concentration

The influence of the CP loading on the photocatalytic reaction is an important parameter, both from a mechanistic and application point of view. For comparison purposes, the CP concentration before the dark adsorption period was varied from 10 to 50 mg L^{-1} for photocatalytic reactions using TiO_2 and CNT-TiO_2 catalysts. In this range of initial concentrations, no significant variation of the initial pH was observed (pH 5.60 ± 0.10). Results showed that for this range of concentrations the reaction rate got slower as the initial amount of phenol in solution increased (Figure 4). The CNT-TiO_2 catalyst showed better photocatalytic efficiency in the whole CP concentration range.

As the phenol concentration increased, more reactants and reaction intermediates were adsorbed onto the surface of the photocatalyst. Therefore, the generation of hydroxyl radicals is reduced because there are fewer active sites for the adsorption of hydroxide anions.

The dependence of a photocatalytic reaction rate on the concentration of an organic substrate is been generally described by the Langmuir–Hinshelwood kinetic model:[33]

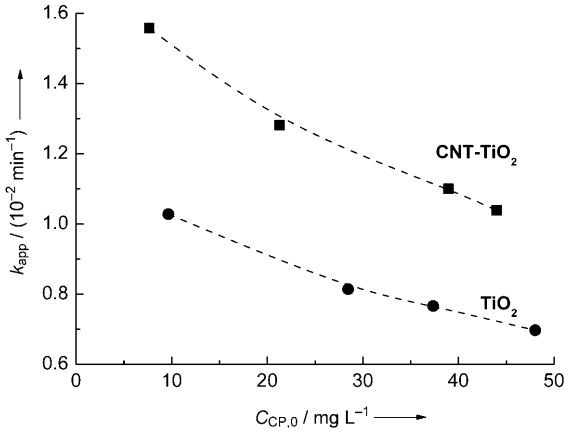

Figure 4. Apparent first-order kinetic rate constant as a function of the initial CP concentration for TiO_2 and CNT-TiO_2 catalytic systems.

$$-r_A = k_{LH}\frac{K_{LH}C_A}{1 + K_{LH}C_A} \quad (8)$$

where r_A is the rate of degradation of the organic compound *A*, and k_{LH} and K_{LH} are the apparent reaction rate and the Langmuir adsorption constants, respectively. Although this is well established and greatly used by many authors to describe the kinetics of photo-oxidation reactions, some considerations have to be taken into account. A pseudo-steady state approach has been proposed by some authors, considering the dependency of the constants k_{LH} and K_{LH} on the light intensity.[40–43] K_{LH} in a photocatalytic oxidation reaction does not have the same meaning as the dark adsorption constant (K_{ads}). In photo-induced reactions, the number of active catalyst sites is much lower than the total number of surface adsorption sites. Thus, the K_{LH} value measured under illumination does not characterize the generally accessible surface probed by dark adsorption measurements. Another fact is that the active sites exist only under illumination and the species involved do not exist to an appreciable level in the dark. In addition, the rate-determining step of the photocatalytic reaction involves the reaction of the adsorbed substrate with photogenerated $HO^{\bullet}$ radicals. Because the latter will be a function of the absorbed light intensity, which in turn will be proportional to the incident light intensity, it follows that k_{LH} will also be a function of absorbed light intensity. In the present work, a medium-pressure mercury lamp was used, with the most important emission line at 366 nm. The photon flux for this wavelength, determined by potassium ferrioxalate actinometry, was 2.38×10^{-6} E s^{-1}.

The values of the Langmuir–Hinshelwood adsorption equilibrium constant, K_{LH}, and the rate constant, k_{LH}, were obtained by adjusting the experimental points to Equation (8). The values were $K_{LH} = 1.38 \times 10^{-2}$ L mg^{-1} and $k_{LH} = 8.37 \times 10^{-1}$ mg L^{-1} min^{-1} for photocatalytic reactions with TiO_2 and $K_{LH} = 1.47 \times 10^{-2}$ L mg^{-1} and $k_{LH} = 1.17$ mg L^{-1} min^{-1} when the CNT-TiO_2 composite catalyst was used. While the kinetic rate constant increased (relative to the TiO_2-only situation), the values of K_{LH} were comparable in the cases of TiO_2 and CNT-TiO_2, suggesting that the thermodynamics of adsorption are similar, the difference being in the kinetics of the process. The conclusion is that the CNTs do not dramatically change the adsorption properties of the resulting catalyst with relation to the initial pollutant molecule, but they play an important role in the kinetics of the photocatalytic process. The role played by CNTs in a composite catalyst has been discussed in previous works using similar materials,[16,24,25] being ascribed to the action of CNTs as a photosensitizer rather then a co-adsorbent or a dispersing agent. After being irradiated, CNTs inject electrons into the conduction band of TiO_2. This triggers the formation of very reactive $HO^{\bullet}$ radicals, which are responsible for the degradation of the organic molecule.

Catalyst reuse

The possibility of catalyst recovery and reuse in further catalytic cycles is of great importance, because it can contribute sub-

stantially to the lowering of operational costs and at the same time reduce the possible negative environmental impact that would result from disposal and/or elimination of the used material.

Fresh CNT-TiO_2 catalyst was used in a first photodegradation experiment (1st run). At the end of two hours of irradiation, the catalyst was separated by centrifugation and reused in a second reaction using a new solution of CP (2nd run). The process was repeated in a consecutive experiment, again using a fresh 50 mg L^{-1} CP solution (3rd run). As shown in Figure 5, the

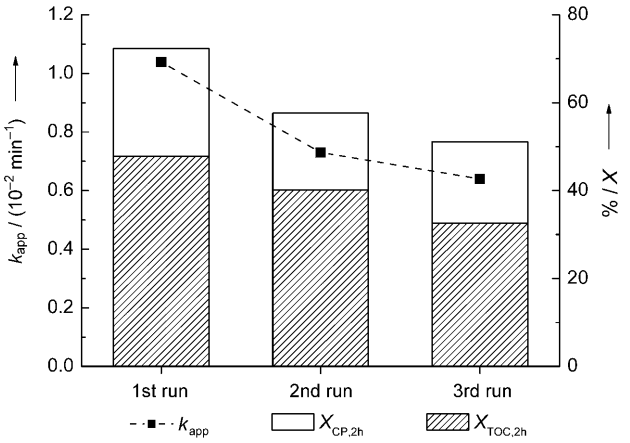

Figure 5. Apparent first-order rate constant (k_{app}), CP conversion ($X_{CP,2h}$) and TOC removal ($X_{TOC,2h}$) during photocatalytic degradation over fresh (1st run) and recovered (2nd and 3rd runs) CNT-TiO_2 suspensions.

catalyst efficiency declined when used in successive reactions. The apparent rate constant decreased by 30% from the 1st to the 2nd photodegradation runs, and a smaller decrease of about 12% from the 2nd to 3rd reuse was observed. This tendency was also observed for CP conversion and TOC removal at the end of each reaction.

The observed loss of photocatalyst efficiency can be due to the presence of reaction intermediates adsorbed onto the active sites of the catalyst. Concurrently, mechanical stress of the catalyst particles can occur because the suspensions were magnetically stirred. Both factors account for a reduction of the number of available photoactive sites and therefore for a decease in the ability of the catalyst to photodecompose CP.

Photocatalytic degradation of *para*-substituted phenolic compounds

The photocatalytic degradation of four *para*-substituted phenol derivatives, that is, 4-aminophenol (AP), 4-chlorophenol (CP), 4-hydroxybenzoic (HBA) acid, and 4-nitrophenol (NP) was performed under near-UV to visible irradiation with TiO_2 and CNT-TiO_2 catalysts. Direct photochemical degradation of the organic compounds was also carried out for comparison. Figure 6 shows UV/Vis absorption spectra of the organic compounds and catalysts. As expected, TiO_2 showed a characteristic sharp absorption edge, rising at 400 nm. The introduction of the carbon phase into the TiO_2 matrix led to an increase of

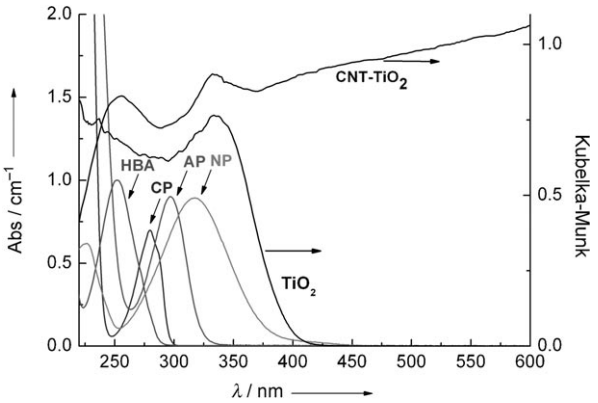

Figure 6. Diffuse reflectance and absorption UV/Vis spectra of the catalysts and of the organic compounds, respectively.

the light absorption, mainly in the visible region of the spectrum. The optical spectra of the organic compounds showed absorptions at wavelengths lower than 400 nm.

The photocatalytic reactivity of aromatic compounds can be affected by the number of substituents, their electronic nature, and their position on the aromatic ring.[44] Some studies have shown that organic molecules that contain electron-donor substituents are easily degraded by photocatalytic oxidation processes.[45,46] The effect that a substituent has on the electronic character of a given aromatic system is represented by the Hammett constant (σ). By definition, hydrogen *para*-substituted phenol is taken as reference, with $\sigma_p = 0$. A modified Hammett constant (σ_p^-) is normally used for situations in which the substituent enters into some resonance with the reaction center in an electron-rich transition state, which is the case for reactions involving phenols.[47] Electron-donating groups, such as $-NH_2$, $-OH$, and $-OCH_3$ show negative Hammett constants, while for electron-withdrawing groups such as $-NO_2$, $-COOH$, $-Cl$, and $-CN$, $\sigma_p^- > 0$. The Hammett constants for AP, CP, HBA, and NP are given in Table 5. Among the studied compounds, 4-aminophenol has the lowest Hammett constant ($\sigma_p^- = -0.66$), which means that is the most electrophilic molecule, while 4-nitrophenol shows a σ_p^- value of 1.25, confirming the deactivating nature of the $-NO_2$ group.

Photochemical and photocatalytic degradation reactions were performed in the absence of catalyst and with TiO_2 or CNT-TiO_2 catalysts, respectively. For all compounds, the photodegradation reactions fit well a pseudo-first-order kinetic rate model. Apparent rate constants obtained for the photochemical and photocatalytic degradation of the four *para*-substituted phenols are listed in Table 5. During the direct photodegradation of AP, the solution passed from colorless to brown, indicating a polymerization process, probably by formation of dihydroxyazobenzene species. Direct photolysis of HBA did not produce any degradation of the initial compound, because it does not absorb within the range in which the aqueous solution was being irradiated. Despite showing residual absorption in the visible range of the spectrum, photodegradation of AP in the absence of catalyst was observed and 53.7% of conversion of the organic molecule at the end of 2 h of irradiation

Table 5. Hammett constant (σ_p^-), apparent first-order kinetic rate constant (k_{app}), synergy factor (R), conversion (X_{2h}), and TOC removal ($X_{TOC,2h}$) after 2 h of irradiation, obtained for the photochemical and photocatalytic degradation of AP, CP, HBA, and NP.

Compound (pK_a)	σ_p^-	Catalyst	k_{app} [$\times 10^{-2}$ min^{-1}]	R	X_{2h} [%]	$X_{TOC,2h}$ [%]
[a]		[a]	n.a.[b]	–	n.a.[b]	n.a.[b]
AP (5.48)	−0.66	TiO_2	0.830	2.21	47.1	5.10
		CNT-TiO_2	1.832	–	59.6	7.70
		[a]	0.593	–	53.7	2.20
CP (9.41)	0.23	TiO_2	0.690	1.51	54.6	42.5
		CNT-TiO_2	1.039	–	72.3	47.4
		[a]	n.a.[c]	–	n.a.[c]	n.a.[c]
HBA (4.57)	0.73	TiO_2	0.613	1.07	49.3	37.5
		CNT-TiO_2	0.660	–	53.8	47.5
		[a]	0.170	–	4.90	1.00
NP (7.15)	1.25	TiO_2	0.460	0.70	23.4	20.9
		CNT-TiO_2	0.320	–	15.6	12.6

[a] Blank experiment. [b] Precipitate formation. [c] No HBA degradation.

was observed. However, only 2% of TOC reduction was achieved, indicating that most of the initial organic content was still present in the treated solution. In the case of NP, although it shows absorption in the near-UV range with a maximum at $\lambda = 317$ nm, very little degradation was observed, with only 4.9% of NP being converted at the end of the reaction. This result is associated to the strong deactivating nature of the $-NO_2$ group.

Although each of the four *para*-substituted phenols showed different degrees of conversion, the photocatalytic process revealed to be much more efficient than the pure photochemical reaction. For each compound the concentration after the dark adsorption period was determined in the presence of TiO_2 or CNT-TiO_2, and the corresponding initial reaction rate (r_0) was calculated. Then, the Hammett constants were correlated with initial degradation rates for the different organic compounds. A plot of r_0 as a function of σ_p^- is shown in Figure 7, for photocatalytic reactions using both TiO_2 and CNT-TiO_2 catalysts.

The good correlation observed between σ_p^- and r_0 for the different compounds indicate the electrophilic nature of the photocatalytic reaction. The photocatalytic degradation rates are in a good degree dependant on the effect of the substituents on the aromatic ring; being accelerated by electron-donating groups (e.g., $-NH_2$ in AP) and retarded by electron-withdrawing substituents (e.g., −Cl, −COOH, and $-NO_2$ in CP, HBA, and NP, respectively). For each category of substituents, the effect on the photodegradation depends on the activating or deactivating ability of each substituent, which is directly related to the value of σ_p^- as shown in Figure 7.

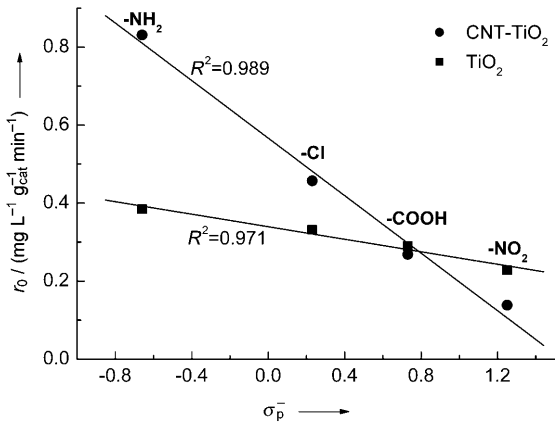

Figure 7. Relationship between initial degradation rate (r_0) and Hammett constant (σ_p^-) for the different *para*-subtituted phenols.

The effect of the introduction of CNTs into the composite catalyst was quantified by means of a synergy factor (R), previously suggested in the literature and defined as $R = k_{app,CNT\text{-}TiO2}/k_{app,TiO2}$ (Table 5).[48] The highest value was obtained for AP ($R = 2.21$), which means a double k_{app} value when composite catalyst was used. The CNT-TiO_2 catalyst also showed a higher efficiency than TiO_2 alone for the degradation of CP, with a 50% increase in k_{app}. For HBA and NP different results were obtained. Apparent first-order kinetic rate constants obtained for the photocatalytic degradation of HBA with CNT-TiO_2 and TiO_2 catalysts were similar, and therefore no kinetic synergy effect was observed for this compound. Nevertheless, in terms of mineralization a higher TOC removal was achieved when the composite catalyst was used. In the case of NP, a lower k_{app} was obtained for the photocatalytic reaction with CNT-TiO_2. This result can be explained by the high deactivating nature of the NP molecule. Although adsorption of NP is greater in the CNT-TiO_2 catalyst than in TiO_2 ($C_{0,NP\text{-}TiO2} = 49.5$ mg L^{-1} and $C_{0,NP\text{-}CNT\text{-}TiO2} = 43.2$ mg L^{-1}), the organic molecule resists attack by hydroxyl radicals at the catalyst surface, leading to a decrease in the efficiency of the photodegradation process. From the above results, it can be concluded that no benefit from the use of a CNT-TiO_2 composite catalyst was observed for *p*-substituted phenols with Hammett constants higher than corresponding to the crossing point of the two straight lines represented in Figure 7, that is, for molecules with $\sigma_p^- > 0.79$.

Reaction mechanism and intermediates

HPLC analysis of the samples collected during the photocatalytic degradation of AP, NP, and CP revealed that the main reaction intermediates were hydroquinone and benzoquinone. Trace concentrations of 4-nitrocatechol and 4-chlorocatechol were detected as degradation intermediates of NP and CP, respectively (Figure 8a and b). The main HBA degradation intermediate was found to be 3,4-hydroxybenzoic acid. Also, very low concentrations of hydroquinone and benzoquinone were detected.

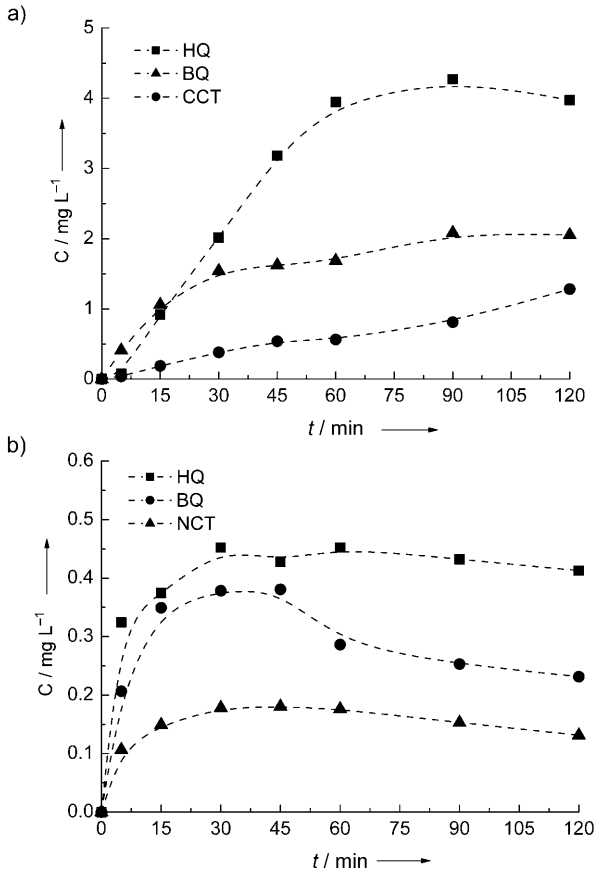

Figure 8. Concentrations of main intermediates during the photocatalytic degradation of a) CP and b) NP using the CNT-TiO_2 catalyst. HQ: hydroquinone; BQ: benzoquinone; CCT: 4-chlorocatechol; NCT: 4-nitrocatechol.

Nitrates were also detected as byproducts of NP photocatalytic degradation. No nitrites were found in the samples, probably because the expected NO_2^- ions were converted into NO_3^- under the strong oxidizing conditions. In the case of AP, ammonium ions should be expected as byproducts of the deamination of the starter molecules. Because the reaction takes place at a pH lower than the pK_a of NH_4^+ (pK_a = 9.27), ammonia occurred mostly as ammonium ion (NH_4^+) instead of NH_3. However, negligible amounts of NH_4^+ were measured and NO_3^- was detected as main byproduct, meaning that ammonium was oxidized to nitrate under the reaction conditions. Despite not being quantified in this work, taking into account the detected intermediates Cl^- was expected to be a byproduct of the photocatalytic degradation of CP.[49] A simplified photocatalytic degradation mechanism of the studied *para*-substituted phenols is shown in Scheme 1.

Following these results it can be stated that hydroxyl radicals are the key species responsible for the degradation of the studied compounds. Hydroquinone is formed when the attack of the HO$^\bullet$ radical takes place at the *para* position, by abstraction of the substituent group. Benzoquinone was also detected as one of the intermediate products, resulting from the degradation of hydroquinone. Simultaneously, benzoquinone can be reduced to hydroquinone by reaction with the electrons from the conduction band of the semiconductor, establishing a

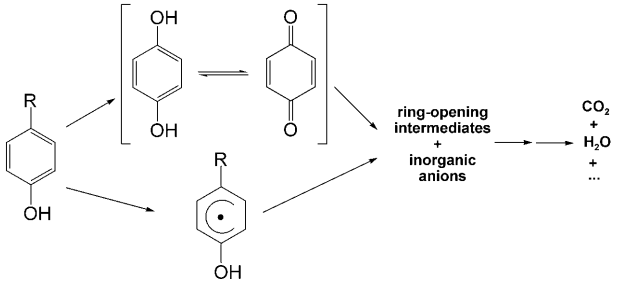

Scheme 1. Simplified photocatalytic degradation mechanism of *para*-substituted phenols.

keto–enolic tautomer oxidoreductive equilibrium.[50] On the other hand, hydroxyl radical can attack the aromatic ring by addition of a hydroxyl group followed by the elimination of a hydrogen atom. The position of the insertion of the hydroxyl group follows the orientating properties of benzene substituent groups. Therefore, 4-chlorocatechol, 4-nitrocatechol, and 3,4-dihydroxybenzoic acid were found as reaction intermediates from CP, NP, and HBA degradation, respectively.

Conclusions

The composite CNT-TiO_2 catalyst produced by a modified acid-catalyzed sol–gel procedure promotes the efficient photocatalytic degradation of *para*-substituted phenols under near-UV to visible irradiation. The preparation procedure leads to a material composed of TiO_2 anatase crystallites of 8.3 nm on the surface of CNTs. The resulting material shows a higher surface area than pure anatase TiO_2, resulting from the action of CNTs as a dispersing media for TiO_2 nanoparticles. There is a strong interphase interaction between carbon and semiconductor phases, as confirmed by the changes in the UV/Vis spectrum of the TiO_2 matrix after the introduction of CNTs.

The use of 4-chlorophenol as model compound to study the effect of operation parameters on the photoefficiency of the degradation reaction in the presence of CNT-TiO_2 catalyst leads to the following findings and conclusions: (1) The optimal catalyst concentration is 1.2 g L^{-1}. (2) At natural pH conditions (pH 5.6) an optimal compromise between kinetic and mineralization photoefficiency of CNT-TiO_2 catalyst can be achieved. (3) Hydrogen peroxide plays a dual role in the photocatalytic process: the introduction of low concentrations of H_2O_2 in the reaction medium leads to a decrease in the efficiency of the degradation process, attributed to the action of H_2O_2 as HO$^\bullet$ radical scavenger. With increasing H_2O_2 concentration the apparent first-order constant tends to gradually increase as a result of the increased relative importance of its role as electron acceptor and hydroxyl radical generator. (4) The reutilization of the recovered CNT-TiO_2 catalyst results in a gradual decrease in the efficiency of the catalyst. (5) A Langmuir-Hinshelwood model, based on a pseudo-steady state approach, can successfully be used to represent the dependency of the photocatalytic reaction rate on the concentration of CP for both TiO_2 and CNT-TiO_2 catalysts.

CNT-TiO_2 was used for the photocatalytic degradation of *para*-substituted phenols to test the effect of the electronic nature of the substituents: (1) The initial degradation rate tends to increase with increasing electronic density on the aromatic ring in the following order: 4-nitrophenol < 4-hydroxybenzoic acid < 4-chlorophenol < 4-aminophenol. (2) The Hammett constant is an adequate descriptor of the photocatalytic degradability of the studied *para*-substituted phenols by using both TiO_2 and CNT-TiO_2 catalysts.

The effect of the introduction of CNT into the TiO_2 matrix was quantified in terms of a synergy factor: (1) The synergy factor was inversely proportional to the Hammett constant of the studied molecules. (2) For AP and CP the use of a CNT-TiO_2 composite catalyst has a beneficial effect on the photoefficiency of the degradation process; conversely, for HBA practically no synergy effect is observed while for NP the use of CNT-TiO_2 results in a negative synergy effect. (3) The photoefficiency of the catalysts is not only related to its intrinsic properties but also to the activating/deactivating nature of the degradation substrate. (4) Hydroquinone and benzoquinone are reaction intermediates for all compounds; also, 4-chlorocatechol, 4-nitrocatechol, and 3,4-dihydroxybenzoic acid are CP, NP, and HBA degradation intermediates, respectively.

Experimental Section

Catalyst production

Multiwalled carbon nanotubes, synthesized by catalytic decomposition of CH_4, were purchased from Shenzhen Nanoport Co. Ltd (manufacturer data: purity > 95%, diameter < 10 nm; length 5–15 μm). TiO_2 and CNT-TiO_2 composite catalysts were prepared by using an acid-catalyzed sol–gel method starting from an alkoxide precursor. The preparation was performed at room temperature as follows: Firstly, 0.1 mol of $Ti(OC_3H7)_4$ (Aldrich, 97%) was dissolved in 200 mL ethanol. The solution was stirred magnetically for 30 min, and then 1.56 mL of nitric acid (Fluka, 65%) was added. The mixture was loosely covered and kept stirring until a homogenous gel formed. The gel was aged in air for several days, and the obtained xerogel was crushed into a fine powder. The CNT-TiO_2 composite catalyst was produced using a CNT/TiO_2 weight ratio of 1:5. The procedure was similar to that described above for pure TiO_2, with CNTs being introduced into a $Ti(OC_3H_7)_4$ ethanol solution. The resulting powders were calcined at 673 K under a flow of N_2 for 2 h to obtain TiO_2 or CNT-TiO_2.

Characterization techniques

XRD patterns were obtained on a Philips X'Pert MPD diffractometer (Cu $K_\alpha = 0.15406$ nm). The thermal behavior of the materials was investigated by thermogravimetric (TG) analysis, using a Mettler TA 4000 instrument equipped with a TG 50 and TC 11-TA system. The runs were carried out under N_2 or air flow using a heating rate of 5 K min^{-1}. N_2 adsorption–desorption isotherms were measured by using a Coulter Omnisorp 100 CX apparatus and the surface area was calculated by the BET method. TEM was performed on a Leica LEO 906E instrument operating at 120 kV. The samples were previously dispersed in ethanol. SEM was performed in a high resolution (Schottky) FEI Quanta 400FEG microscope. Elemental analysis was determined by EDX in an EDAX Genesis X4 M apparatus. The UV/Vis spectra of the powder solids were measured on a JASCO V-560 UV/Vis spectrophotometer, equipped with an integrating sphere attachment (JASCO ISV-469). The powder samples were diluted in $BaSO_4$ using a mass ratio of 1:3.

Photocatalytic degradation experiments

The photocatalytic degradations of four phenolic compounds, 4-chlorophenol (CP, Aldrich, 99+%), 4-aminophenol (AP, Aldrich, 98+%), 4-nitrophenol (NP, Aldrich, 98%), and 4-hydroxybenzoic acid (HBA, Fluka, ≥99%), were performed in aqueous solutions under near-UV to visible irradiation. The experiments were carried out in a 300 mL glass immersion photochemical reactor charged with 250 mL of solution/suspension. The reactor was equipped with a Heraeus TQ 150 medium-pressure mercury vapor lamp (more intense lines at λ_{exc} of 366, 436, and 546 nm; the UV line at 254 nm being filtered by a DURAN 50 glass jacket), which was located axially and held in a quartz immersion tube. The initial concentration of the substrates was set at 50 mg L^{-1}. A 200 mL min^{-1} oxygen/argon (20% vol. of oxygen) stream was continuously supplied to the reactor. Reactions took place under natural pH (pH_{nat}) conditions ($pH_{nat,CP} = 5.6$; $pH_{nat,AP} = 6.6$; $pH_{nat,NP} = 5.4$; $pH_{nat,HBA} = 4.0$). Before switching on the illumination, the suspensions were saturated with the gas mixture and magnetically stirred for 30 min to establish an adsorption–desorption equilibrium. The first sample was taken at the end of the dark adsorption period, just before the light was switched on, to determine the concentration of the compound in bulk solution, which was thereafter considered the initial concentration (C_0) after dark adsorption. The suspensions were then irradiated at constant stirring speed. Reactions were normally stopped after 2 h of irradiation. During irradiation samples were withdrawn regularly from the reactor, and centrifuged prior to analysis to separate any suspended solids.

Analytical methods

The clean transparent solutions were analyzed by HPLC using a Hitachi Elite LaChrom liquid chromatograph equipped with an L-2450 diode array detector. The stationary phase consisted of a YMC-Pack ODS-AQ end-capped column (250 mm × 4.6 mm, 5 μm particles) working at room temperature. The mobile phase was a mixture of a 20 mM NaH_2PO_4/H_3PO_4 (pH 2.8) buffer solution and acetonitrile with a gradient concentration at a flow rate of 1 mL min^{-1}. For known compounds, the relationship between area and concentration was determined by using standards. The concentration of ammonium ions (NH_4^+) in samples was determined by the 4500-NH_3 ammonia-selective electrode method.[51] Total organic carbon measurements were performed in a Shimadzu TOC-5000 analyzer.

Acknowledgements

This research was carried out by projects SFRH/BD/16966/2004, POCI/EQU/58252/2004, POCTI/1181/2003, approved by the FCT, Programa Operacional (POCTI/POCI) and co-supported by FEDER. We are indebted to Dr. Pedro Tavares (UTAD) for technical assistance and advice with TEM measurements.

Keywords: composites · heterogeneous catalysis · nanotubes · photochemistry · titanium

[1] R. Andreozzi, V. Caprio, A. Insola, R. Marotta, *Catal. Today* **1999**, *53*, 51 – 59.
[2] P. R. Gogate, A. B. Pandit, *Adv. Environ. Res.* **2004**, *8*, 501 – 551.
[3] P. R. Gogate, A. B. Pandit, *Adv. Environ. Res.* **2004**, *8*, 553 – 597.
[4] M. Pera-Titus, V. García-Molina, M. A. Baños, J. Giménez, S. Esplugas, *Appl. Catal. B: Environm.* **2004**, *47*, 219 – 256.
[5] U. I. Gaya, A. H. Abdullah, *J. Photochem. Photobiol. C* **2008**, *9*, 1 – 12.
[6] G. Palmisano, V. Augugliaro, M. Pagliaro, L. Palmisano, *Chem. Commun.* **2007**, 3425 – 3437.
[7] A. Fujishima, T. N. Rao, D. A. Tryk, *J. Photochem. Photobiol. C* **2000**, *1*, 1 – 21.
[8] Y. Gao, Y. Masuda, W.-S. Seo, H. Ohta, K. Koumoto, *Ceram. Int.* **2004**, *30*, 1365 – 1368.
[9] H.-I. Hsiang, S.-C. Lin, *Mater. Chem. Phys.* **2006**, *95*, 275 – 279.
[10] S. S. Watson, D. Beydoun, J. A. Scott, R. Amal, *Chem. Eng. J.* **2003**, *95*, 213 – 220.
[11] S. Anandan, M. Yoon, *J. Photochem. Photobiol. C* **2003**, *4*, 5 – 18.
[12] M. Anpo, M. Takeuchi, *J. Catal.* **2003**, *216*, 505 – 516.
[13] E. P. Reddy, L. Davydov, P. Smirniotis, *Appl. Catal. B: Environm.* **2003**, *42*, 1 – 11.
[14] C. G. da Silva, J. L. Faria, *J. Photochem. Photobiol. A* **2003**, *155*, 133 – 143.
[15] B. Tryba, A. W. Morawski, M. Inagaki, *Appl. Catal. B: Environm.* **2003**, *41*, 427 – 433.
[16] W. Wang, P. Serp, P. Kalck, J. L. Faria, *Appl. Catal. B: Environm.* **2005**, *56*, 305 – 312.
[17] W. D. Wang, C. G. Silva, J. L. Faria, *Appl. Catal. B: Environm.* **2007**, *70*, 470 – 478.
[18] S. Iijima, *Nature* **1991**, *354*, 56 – 58.
[19] P. Serp, M. Corrias, P. Kalck, *Appl. Catal. A: Gen.* **2003**, *253*, 337 – 358.
[20] W. Feng, Y. Y. Feng, Z. G. Wu, A. Fujii, M. Ozaki, K. Yoshino, *J. Phys. Condens. Matter* **2005**, *17*, 4361 – 4368.
[21] B. Gao, G. Z. Chen, G. L. Puma, *Appl. Catal. B: Environm.* **2009**, *89*, 503 – 509.
[22] S. L. Kim, S. R. Jang, R. Vittal, J. Lee, K. J. Kim, *J. Appl. Electrochem.* **2006**, *36*, 1433 – 1439.
[23] Y. Ou, J. D. Lin, S. M. Fang, D. W. Liao, *Chem. Phys. Lett.* **2006**, *429*, 199 – 203.
[24] W. Wang, P. Serp, P. Kalck, J. L. Faria, *J. Mol. Catal. A: Chem.* **2005**, *235*, 194 – 199.
[25] W. Wang, P. Serp, P. Kalck, C. G. Silva, J. L. Faria, *Mater. Res. Bull.* **2008**, *43*, 958 – 967.
[26] K. Woan, G. Pyrgiotakis, W. Sigmund, *Adv. Mater.* **2009**, *21*, 2233 – 2239.
[27] W. Gernjak, M. I. Maldonado, S. Malato, J. Caceres, T. Krutzler, A. Glaser, R. Bauer, *Sol. Energy* **2004**, *77*, 567 – 572.
[28] H. T. Gomes, J. L. Figueiredo, J. L. Faria, *Catal. Today* **2007**, *124*, 254 – 259.
[29] M. Cristina Yeber, J. Rodriguez, J. Freer, N. Duran, H. D. Mansilla, *Chemosphere* **2000**, *41*, 1193 – 1197.
[30] V. Uvarov, I. Popov, *Mater. Charact.* **2007**, *58*, 883 – 891.
[31] G. Leofanti, M. Padovan, G. Tozzola, B. Venturelli, *Catal. Today* **1998**, *41*, 207 – 219.
[32] K. S. W. Sing, D. H. Everett, R. A. W. Haul, L. Moscou, R. A. Pierotti, J. Rouquérol, T. Siemieniewska, *Pure Appl. Chem.* **1985**, *57*, 603 – 619.
[33] J. M. Herrmann, *Top. Catal.* **2005**, *34*, 49 – 65.
[34] C. G. Silva, W. D. Wang, J. L. Faria, *J. Photochem. Photobiol. A* **2006**, *181*, 314 – 324.
[35] X. H. Li, J. L. Niu, J. Zhang, H. L. Li, Z. F. Liu, *J. Phys. Chem. B* **2003**, *107*, 2453 – 2458.
[36] V. Auguliaro, E. Davi, L. Palmisano, M. Schiavello, A. Sclafani, *Appl. Catal.* **1990**, *65*, 101 – 116.
[37] K. Tanaka, T. Hisanaga, K. Harada, *J. Photochem. Photobiol. A* **1989**, *48*, 155 – 159.
[38] Y. J. Zang, R. Farnood, *Top. Catal.* **2006**, *37*, 91 – 96.
[39] W. Chu, C. C. Wong, *Water Res.* **2004**, *38*, 1037 – 1043.
[40] A. V. Emeline, V. Ryabchuk, N. Serpone, *J. Photochem. Photobiol. A* **2000**, *133*, 89 – 97.
[41] A. Mills, J. Wang, D. F. Ollis, *J. Phys. Chem. B* **2006**, *110*, 14386 – 14390.
[42] D. F. Ollis, *J. Phys. Chem. B* **2005**, *109*, 2439 – 2444.
[43] D. F. Ollis, *Top. Catal.* **2005**, *35*, 217 – 223.
[44] M. H. Priya, G. Madras, *J. Photochem. Photobiol. A* **2006**, *179*, 256 – 262.
[45] G. Palmisano, M. Addamo, V. Augugliaro, T. Caronna, A. D. Paola, E. G. López, V. Loddo, G. Marcì, L. Palmisano, M. Schiavello, *Catal. Today* **2007**, *122*, 118 – 127.
[46] S. Parra, J. Olivero, L. Pacheco, C. Pulgarin, *Appl. Catal. B: Environm.* **2003**, *43*, 293 – 301.
[47] G. W. Gokel, *Dean's Handbook of Organic Chemistry* (2nd Ed.), McGraw-Hill, **2004**.
[48] J. Matos, J. Laine, J.-M. Herrmann, *Appl. Catal. B: Environm.* **1998**, *18*, 281 – 291.
[49] B. Malinowska, J. Walendziewski, D. Robert, J. V. Weber, M. Stolarski, *Appl. Catal. B: Environm.* **2003**, *46*, 441 – 451.
[50] A. G. Rincón, C. Pulgarin, N. Adler, P. Peringer, *J. Photochem. Photobiol. A* **2001**, *139*, 233 – 241.
[51] M. H. Franson, A. D. Eaton, L. S. Clesceri, A. E. Greenberg, *Standard Methods for the Examination of Water and Wastewater*, Washington DC, **2005**.

Received: November 11, 2009
Revised: January 21, 2010
Published online on April 30, 2010

